

# Study on some characteristics of KDP crystals grown by Sankaranarayanan-Ramasamy (SR) and conventional technique

V. T. PHAN\*, A. Q. LE, N. V. LE, D. T. HUYNH

*Faculty of Physics-Engineering Physics, University of Science, Vietnam National University, Ho Chi Minh city 700071, Vietnam*

Sankaranarayanan-Ramasamy (SR) is a technique of crystal growth in an aqueous solution proposed in the year of 2005. SR technique included the Y-shaped solution vessel and the crystal seed at the bottom of the vessel in order to grow a single crystal unidirectionally, which is contrary to conventional technique. This technique has many advantages over conventional technique, such as high-quality grown crystals, the absence of spontaneous crystalline clusters at the bottom of the vessel which make the growth of main single crystal slower, and effective control of growth direction. In this study, Potassium Dihydrogen Phosphates (KDP) crystals were grown by the temperature lowering method with SR technique and conventional technique. The KDP crystals were characterized by Ultraviolet-Visible (UV-Vis) spectroscopy, Fourier-transform infrared (FT-IR) analysis, X-Ray diffraction (XRD) analysis, and measurement of second harmonic generation (SHG) efficiency and nonlinear doubling coefficient. These properties of SR technique grown KDP crystals were compared to conventional ones, that showed the superiority of the new technique.

(Received July 14, 2018; accepted November 29, 2018)

*Keywords:* KDP, Sankaranarayanan-Ramasamy (SR), Temperature lowering method, Second harmonic generation (SHG), Nonlinear optical coefficient

## 1. Introduction

KDP crystal is well-known due to its important applications such as electro-optic modulation, Q-switching [1], frequency doubling and the frequency converter for high-power laser facility [2]. Some of the world's largest laser fusion facilities are the "Gekko-XII" in Japan, the "Laser Mégajoule" (LMJ) in France, and the "National Ignition Facility" (NIF) in the United States [3]. Giant KDP crystals (about  $55 \times 55 \text{ cm}^2$  in cross-section) were grown at the Lawrence Livermore National Laboratory for the specific needs of the NIF. The growth rate of these KDP crystals was 12-15 mm/day along z-axis [4]. This rapid growth technique is based on the temperature lowering method and motion of seed crystal. Moreover, a continuous filtration system was used to avoid spontaneous nucleation in supersaturation solution; therefore the optical quality of the crystals was improved [5]. Many works around the world have used this rapid growth method to study KDP crystal.

Two research tendencies have been interested in order to improve the quality of KDP crystal and its characteristics. Firstly, the doping of various organic and inorganic substances into KDP crystal has been widely investigated. Some of the impurities, such as KCl (Potassium Chloride) and EDTA (Ethylenediaminetetraacetic Acid), improve the structural perfection of crystal by preventing heavy metal ions diffuse into the matrix of KDP crystal [6, 7]. Other impurities, especially dyes (Amaranth, Sunset

Yellow, Crystal Violet, Xylenol Orange, etc.) and amino acids (L-Arginine, L-Alanine, Glycine, etc.) make remarkable changes in habits of the crystal [8-11]. They mostly increase nonlinear coefficients of KDP crystal [12, 13]. Secondly, new methods or techniques have been proposed.

The essential factor for growing a crystal from aqueous solution is the supersaturation state of the mother solution. Supersaturation can be achieved in several ways: the lowering of temperature, the evaporation of a solvent, and solution replenishment [14]. KDP crystals have been grown in their natural shape for a long time. The formation of inclusions in the crystal is inevitable. The inclusions which are vacancies containing trapped solvent will harm structure and quality of crystal. They are formed by various developments of different facets in a crystal [7]. SR technique can fix the problem by the unidirectional growth of the crystal. SR method grown KDP crystals have higher quality and crystalline perfection than conventional ones [15]. Especially, the single crystal can be grown in any desired orientation such as second harmonic direction (SHD) [16].

In this work, single KDP crystals were grown by the temperature lowering method with SR technique and conventional technique, which are abbreviated to "SR KDP crystal" and "conventional KDP crystal" respectively. The best quality crystals were cut and polished to investigate some structural and optical properties, one of which was the SHG effect. The results of SR and conventional KDP crystal are compared.

## 2. Experimental

KDP solution saturated at 50°C KDP was prepared by dissolving 791.35 g commercial KDP powder (purity  $\geq 99.5\%$ ) in 2000 ml distilled water. The solution was heated to about 80°C and then filtered three times to remove almost insoluble impurities. It was poured into two 1000 ml vessels: cylindrical one for conventional technique and Y-shaped one for SR technique. The seed crystal in conventional technique was attached to one end of a glass rod which was hung in the solution (Fig. 1(a)). It could grow freely in all directions. In contrast, the seed crystal in SR technique was restricted in growth directions except for  $\langle 001 \rangle$  direction. The SR KDP seed was mounted upright at the bottom of the Y-shaped vessel (Fig. 1(b)). The vessels were kept inside a 50°C water bath. The temperature of the bath was reduced at the rate of 1°C/day until reaching 20°C. At that time, the single KDP crystals were harvested (Fig. 2 and Fig. 3).

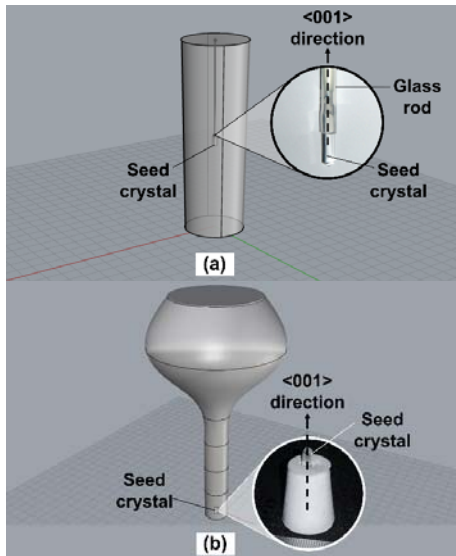


Fig. 1. Schematic of the solution vessel in conventional technique (a) and SR technique (b)

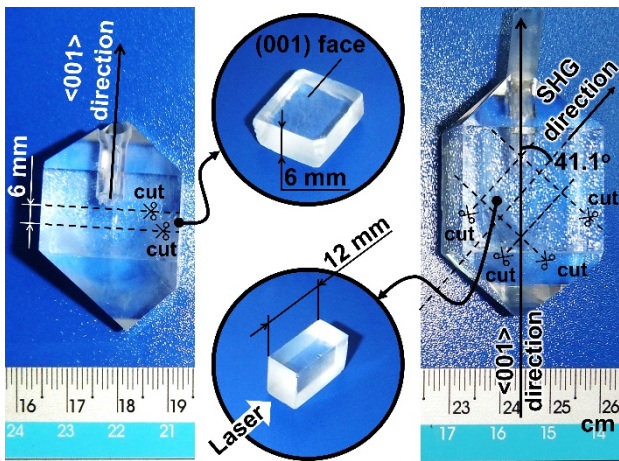


Fig. 2. Conventional single KDP crystals: original shape, 6 mm thick slice, and 12 mm thick piece

Some of KDP crystals were cut into 6 mm thick slices to  $\langle 001 \rangle$  direction. The others were cut into pieces to type I phase-matching angle (41.1°) [17]. The KDP slices were characterized by UV-Vis spectroscopy (HALO RB-10, Dynamica), FT-IR analysis (NICOLET 6700, Thermo), and XRD analysis (D2 PHASER, Bruker) while the KDP pieces were investigated SHG effect.

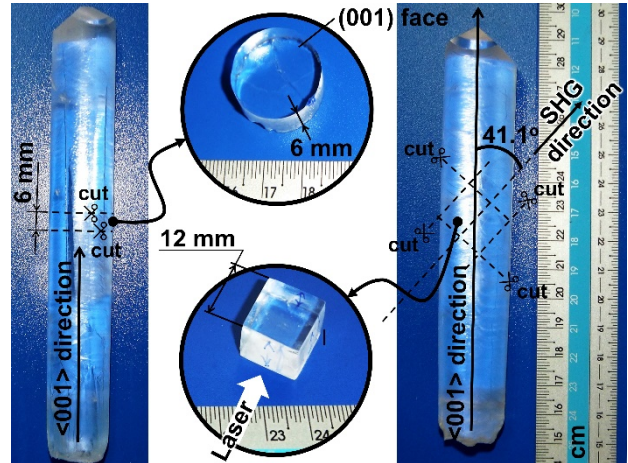


Fig. 3. SR single KDP crystals: original shape, 6 mm thick slice, and 12 mm thick piece

## 3. Results and discussion

### 3.1. UV-Vis spectroscopy

Fig. 4 shows the transmission spectra in the wavelength region 200-1200 nm of SR and conventional KDP crystal. Both the spectra represent high transparency. The transmittance percentage of SR crystal is higher from 16.7 to 20.6% in the visible and near IR region than that of conventional crystal.

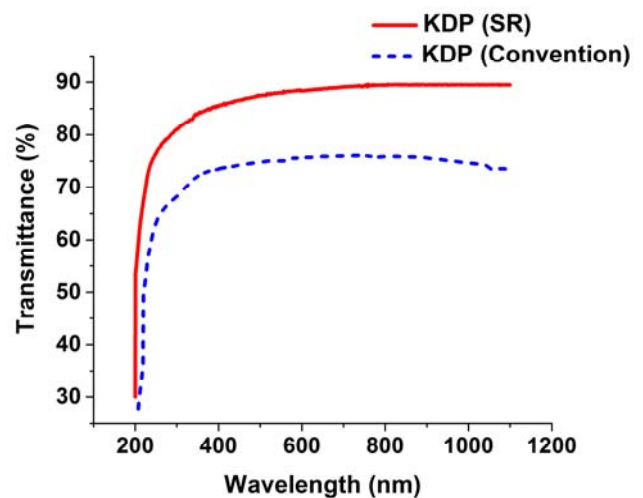


Fig. 4. UV-Vis transmission spectra of SR and conventional KDP crystals

The other important optical quantity is absorption coefficient  $\alpha$  which can be deduced from data of the transmittance by:

$$\alpha = \frac{1}{d} \ln \frac{I_0}{I} \quad (1)$$

where  $T$  is the transmittance and  $d$  is the thickness of the crystal. KDP crystal is a direct transition material [18]. The relation between the absorption coefficient  $\alpha$  and the energy gap  $E_g$  is given by:

$$\alpha = \frac{A(h\nu - E_g)^{1/2}}{h\nu} \quad (2)$$

The linear equation  $y = ax + b$  (where  $y$  is  $(\alpha h\nu)^2$ ,  $x$  is  $h\nu$ ,  $a$  is  $A^2$  and  $b$  is  $-A^2 E_g$ ) of the absorption edge was set to determine the value of  $E_g$ . The parameters  $a$  and  $b$  were defined by the least-squares fitting method based on pairs of  $(h\nu, (\alpha h\nu)^2)$  of the absorption edge (Fig. 5). The value of band energy gap was the intersection between the line  $y = ax + b$  and the  $x$ -axis (Fig. 6). The calculated values of SR and convention KDP crystal's band gap were 5.35 and 5.21 eV, respectively. The band gap is proportional to the Laser-Induced Damage Threshold (LIDT) of nonlinear crystals and inversely proportional to dislocation density in the crystal [15, 19]. Therefore, the SR crystal has higher LIDT and lower dislocation density than the conventional crystal.

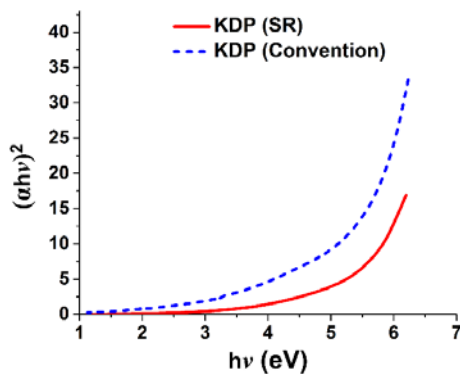


Fig. 5. Plot of  $(\alpha h\nu)^2$  versus photon energy for SR and conventional KDP crystals

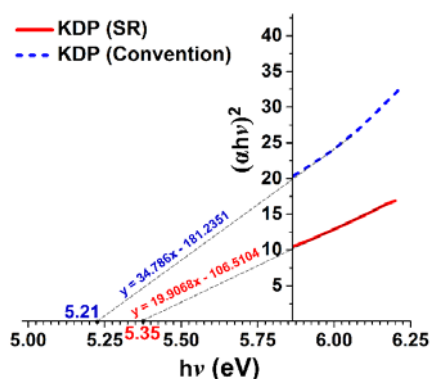


Fig. 6. Plot of straight lines of absorption edge for SR and conventional KDP crystals

### 3.2. FT-IR analysis

FT-IR spectra for the SR and conventional KDP crystals are shown in Fig. 7. The SR KDP graph performed more clear characteristic peaks than the conventional one. There are the strong absorptions at  $538.76 \text{ cm}^{-1}$  (HO-P-OH bending vibration),  $903.88 \text{ cm}^{-1}$  (P-O-H stretching vibration),  $1098.45 \text{ cm}^{-1}$  and  $1301.55 \text{ cm}^{-1}$  (P=O stretching vibration). They are the most important vibrational frequencies of  $\text{PO}_4^{3-}$  anion, which contributes approximately 99% to SHG coefficient [20]. In addition, both peaks at  $1634.11 \text{ cm}^{-1}$  and  $2435.66 \text{ cm}^{-1}$  correspond with the stretching vibration of O=P-OH. The peaks at  $2850.39 \text{ cm}^{-1}$  and  $3440.31 \text{ cm}^{-1}$  show P-O-H asymmetric stretching and O-H stretching vibration, respectively.

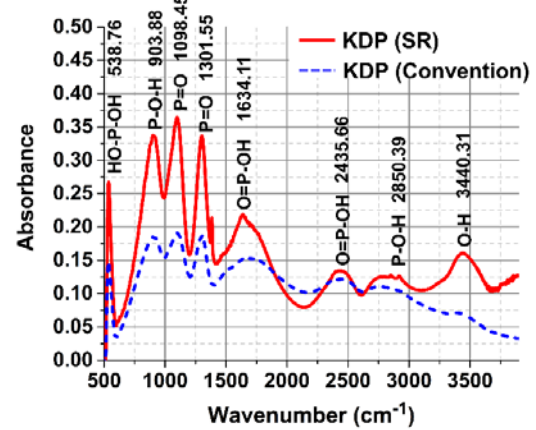


Fig. 7. FT-IR spectra of SR and conventional KDP crystals

Table 1. Observed characteristic IR frequencies of KDP crystal

Wavenumber ( $\text{cm}^{-1}$ )		Assignments [Ref. 21]
SR KDP	Conventional KDP	
538.76 (s)	535 (s)	HO-P-OH bending
903.88 (s)	908 (s)	P-O-H stretching
1098.45 (s)	1106 (s)	P=O stretching
1301.55 (s)	1299 (s)	P=O stretching
1634.11 (m)	1640 (m)	O=P-OH stretching
2435.66 (w)	2437 (w)	O=P-OH stretching
2850.39 (vw)	-	P-O-H asymmetric stretching
3440.31 (vw)	-	O-H stretching

vs - very strong; s - strong; m - medium; w - weak; vw - very weak

### 3.3. Powder XRD analysis

Fig. 8 shows the comparison of powder XRD patterns of SR and conventional KDP crystals. The clearly observed peaks are (101), (200), (211), (112), (220), (202), (301), (103), (321) and (312). There is no change in the peak positions, but SR KDP crystal shows the higher

values in peak intensity than conventional KDP crystal. This result proved SR technique is able to reduce dislocation density or defects in the crystal effectively.

Besides, the XRD data can be used to calculate lattice parameters. Wulff–Bragg's condition with positive integer  $n = 1$ :

$$2 \cdot d_{hkl} \cdot \sin \theta_{hkl} = \lambda \quad (3)$$

where  $\lambda$  is the wavelength of the incident wave, namely  $\lambda = 1.5406 \text{ \AA}$  of Cu  $K\alpha$  radiation in this work,  $d_{hkl}$  is the spacing of (hkl) lattice planes, and  $\theta_{hkl}$  is the angle between the incident ray and (hkl) plane.

KDP has a tetragonal crystal structure whose the interplanar spacing  $d_{hkl}$  is given by:

$$\frac{1}{d_{hkl}^2} = \frac{h^2 + k^2}{a^2} + \frac{l^2}{c^2} \quad (4)$$

From XRD data, Eq. (3) and Eq. (4), the lattice parameters are found out:  $a = b = 7.4477 \text{ \AA}$  and  $c = 6.9749 \text{ \AA}$ . There are no any significant differences between the lattice parameters of SR crystal and conventional crystal. The values are close to statement in Nikogosyan's work ( $a = b = 7.448 \text{ \AA}$  and  $c = 6.977 \text{ \AA}$  at  $T = 296\text{K}$ ) [17].

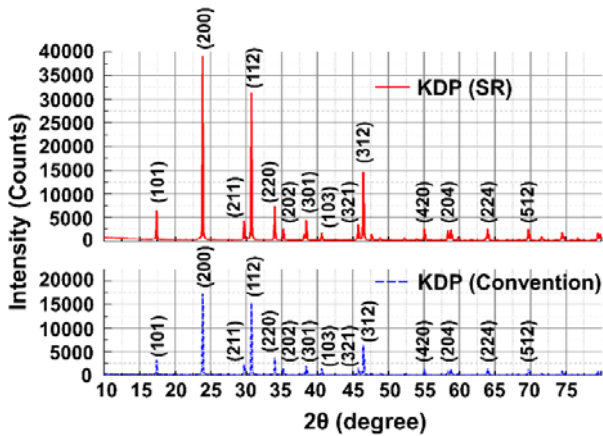


Fig. 8. Powder XRD patterns of SR and conventional KDP crystals

### 3.4. SHG

The 12 mm thick KDP samples directed to type I phase-matching angle ( $41.1^\circ$ ) were investigated SHG effect. The SHG optical system included three main components: the 1064 nm Nd:YAG laser (LSR-PS-II, Lilly Electronics), the 1064 nm filter (OMEGA), and digital laser power meter (SANWA LP1) (Fig. 9). The 1064 nm laser has continuous-wave operation mode and adjustable power from 0 to 1W. The KDP crystal kept between the laser and the 1064 nm filter was turned around the z-axis into the position of brightest green light (532 nm). The green light (or SHG radiation) was recorded by laser power meter.

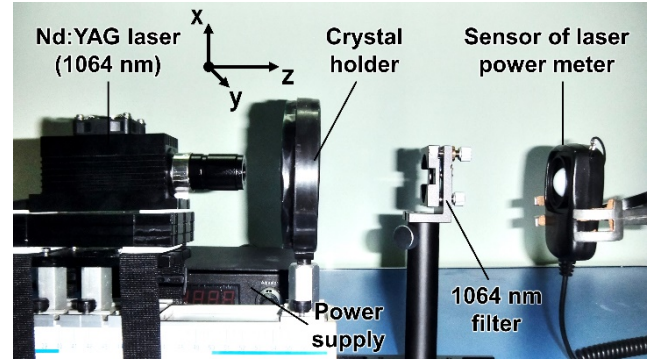


Fig. 9. The optical system for investigating SHG

In order to determine the power of SHG radiation accurately, measurement was performed with a 1064 nm filter and a pair of 1064 nm filters which consists of two identical 1064 nm filters together. A set of two linear equations was established:

$$0.19\% \times P_{1064\text{-in}} + 95.56\% \times P_{532\text{-out}} = P_{1 \text{ filter}} \quad (5a)$$

$$0.02\% \times P_{1064\text{-in}} + 86.26\% \times P_{532\text{-out}} = P_{2 \text{ filters}} \quad (5b)$$

where  $P_{1064\text{-in}}$  and  $P_{532\text{-out}}$  were power of input 1064 nm and output 532 nm SHG radiations respectively,  $P_{1 \text{ filter}}$  and  $P_{2 \text{ filters}}$  were the values recorded by laser power meter with a 1064 nm filter and a pair of 1064 nm filters respectively, and percentage coefficients were transmittance percentages of a 1064 nm filter and a pair of 1064 nm filters at the wavelength of 1064 nm and 532 nm (Fig. 10).

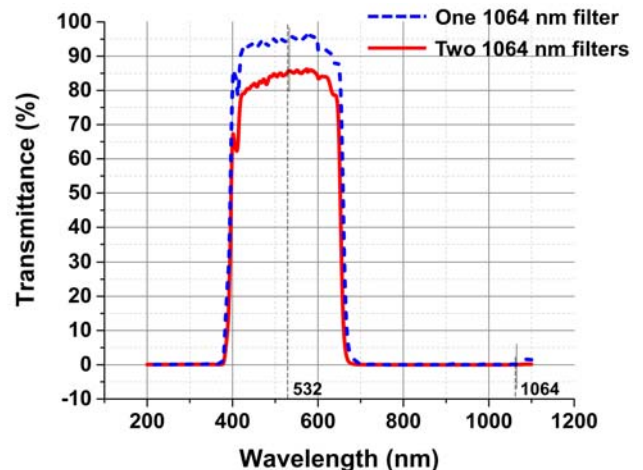


Fig. 10. UV-Vis transmission spectra of a 1064 nm filter and a pair of 1064 nm filters

Amnon Yariv and Pochi Yeh [22] presented a theoretical expression which determines maximum SHG efficiency of the Gaussian beam corresponding to the phase-matching condition:

$$e_{\text{SHG}}^{\text{max}} = \frac{P_{532\text{-out}}}{P_{1064\text{-in}}} = \frac{8}{\pi c} \frac{\alpha \mu_0 \omega^{3/2}}{\xi \epsilon_0} \frac{\omega^3 d^2 L}{n_{1064}^2} P_{1064\text{-in}} \quad (6)$$

where  $c$  is speed of light in vacuum ( $2.9979 \times 10^8$  m/s),  $\epsilon_0$  is vacuum permittivity ( $8.8542 \times 10^{-12}$  F/m),  $\mu_0$  is vacuum permeability ( $4\pi \times 10^{-7}$  H/m),  $\omega$  is angular frequency of input laser ( $\omega = 2\pi c/\lambda$ ),  $d$  is nonlinear coupling coefficient of crystal,  $L$  is length of crystal ( $L = 12$  mm), and  $n_{1064}$  is refractive index of crystal with wavelength of input 1064 nm laser ( $n_{1064} = 1.4937$ ).

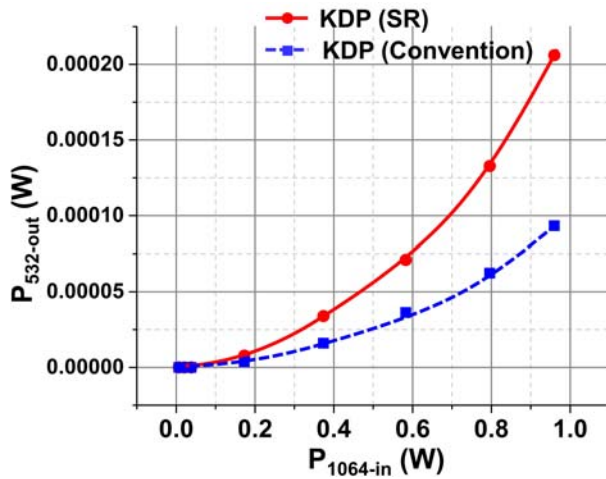


Fig. 11. The powers of SHG radiations of SR and conventional KDP crystals

The power values of SHG radiation and corresponding SHG efficiencies are listed in Table 2. Fig. 11 and 12 show that the results are suitable to Eq. (6). The 532 nm power graph was a half of the parabola, and the SHG efficiency graph was linear. The SHG efficiency of SR KDP crystal was greater than that of conventional crystal about 2.21 times at input laser power of 0.96W.

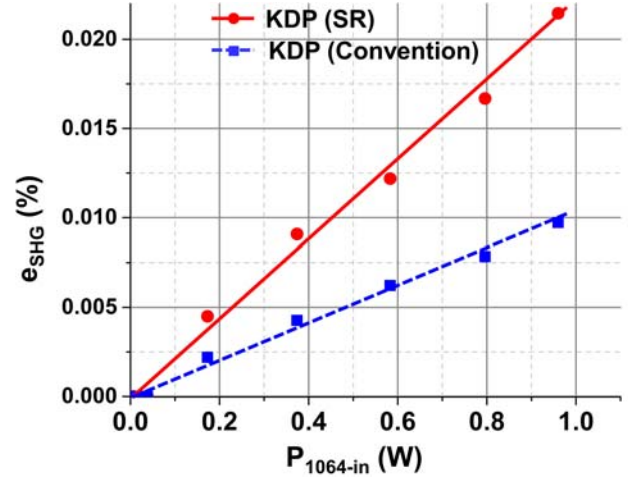


Fig. 12. The SHG efficiencies of SR and conventional KDP crystals

### 3.5. Nonlinear coupling coefficient

Nonlinear coupling coefficient  $d$  depends on the material, the wavelength of the input laser, and phase-matching condition. KDP crystal which is a negative uniaxial crystal satisfies type I phase-matching condition, then  $d = d_{36}$  [22] ( $d_{36}$  is an element of the second-order nonlinear optical coefficient tensor). Here,  $d_{36}$  can be calculated from Eq. (6):

$$d = d_{36} = \sqrt{\frac{P_{532\text{-out}}}{P_{1064\text{-in}}^2} \frac{\pi c}{8} \frac{\alpha \mu_0 \omega^{3/2}}{\xi \epsilon_0} \frac{n_{1064}^2}{\omega^3 L}} \quad (6)$$

Average  $d_{36}$  values of SR and conventional KDP crystals were 0.411 and 0.284 pm/V (Table 2), which are slightly different from that of other works, such as 0.5 pm/V [22], 0.38 pm/V [23]; and 0.38 pm/V, 0.39 pm/V,  $0.39 \pm 0.03$  pm/V, and  $0.40 \pm 0.02$  pm/V [17]. SR KDP crystal has higher  $d_{36}$  coefficient compared to conventional KDP crystal.

Table 2. SHG radiation powers, SHG efficiencies, and nonlinear coupling coefficients of SR and conventional KDP crystals

$P_{1064\text{-in}}$ (W)	SR KDP crystal			Conventional KDP crystal		
	$P_{532\text{-out}}$ (W) $\times 10^{-6}$	$e_{\text{SHG}}$ (%)	$d$ (pm/V)	$P_{532\text{-out}}$ (W) $\times 10^{-6}$	$e_{\text{SHG}}$ (%)	$d$ (pm/V)
0	0	-	-	0	-	-
0	0	-	-	0	-	-
0.007	0	0	-	0	0	-
0.021	0	0	-	0	0	-
0.038	0	0	-	0	0	-
0.173	7.7677	0.00449	0.438	3.7887	0.00219	0.306
0.374	33.9592	0.00908	0.424	15.9324	0.00426	0.29
0.583	71.0094	0.01218	0.393	36.2626	0.00622	0.281
0.796	132.773	0.01668	0.394	62.3268	0.00783	0.27
0.96	206.016	0.02146	0.406	93.312	0.00972	0.273
- Non-existence		Average:	0.411		Average:	0.284

#### 4. Conclusions

Single KDP crystals have been grown by the temperature lowering method with conventional technique and SR technique. Some characteristics of the crystals were studied by UV-Vis spectroscopy, FT-IR analysis, powder X-ray diffraction, second harmonic generation (SHG), and calculation of nonlinear coupling coefficient.

The crystal grown by SR technique is found in higher optical transmission and more perfect crystalline structure than the crystal grown by conventional technique. That's what leads to higher SHG efficiency and nonlinear optical coefficient of SR KDP crystal compared to conventional KDP crystal.

SR technique should develop widely in the future due to the ability to provide high-quality single crystals. This study will be helpful to enhance the quality of KDP crystal for various applications.

#### References

- [1] L. Xinju, *Laser Technology*, CRC Press, Boca Raton, Florida, USA, 427 (2010).
- [2] P. Rudolph, *Crystal Growth Technology Semiconductors and Dielectrics*, Wiley-VCH, Weinheim, Germany, 366 (2010).
- [3] J. Leroudier, J. Zaccaro, M. Ildefonso, S. Veessler, J. Baruchel, A. Ibanez, *Cryst. Growth Des.* **11**, 2592 (2011).
- [4] N. Zaitseva, L. Carman, *Progress in Crystal Growth and Characterization of Materials* **43**, 1 (2001).
- [5] N. Zaitseva, J. Atherton, R. Rozsa, L. Carman, I. Smolsky, M. Runkel, R. Ryon, L. James, *J. Cryst. Growth* **197**, 911 (1999).
- [6] H. Dizaji, A. Roust, *Optik* **127**, 11336 (2016).
- [7] A. Ghane, H. Dizaji, *Chinese Journal of Physics* **50**, 652 (2012).
- [8] P. Rajesh, A. Silambarasan, P. Ramasamy, *Mater. Res. Bull.* **49**, 640 (2014).
- [9] S. Chandran, R. Paulraj, P. Ramasamy, *Mater. Chem. Phys.* **186**, 365 (2017).
- [10] F. Akhtar, J. Podder, *Journal of Crystallization Process and Technology* **1**, 55 (2011).
- [11] K. D. Parikh, D. J. Dave, B. B. Parekh, M. J. Joshi, *Bull. Mater. Sci.* **30**, 105 (2007).
- [12] M. Shkir, V. Ganesh, N. Vijayan, B. Riscob, A. Kumar, D. K. Rana, M. S. Khan, M. Hasmuddin, M. A. Wahab, R. R. Babu, G. Bhagavannarayana, *Spectrochim Acta Part A* **103**, 199 (2013).
- [13] E. F. Dolzhenkova, E. I. Kostenyukova, O. N. Bezkravnaya, I. M. Pritula, *J. Cryst. Growth* **478**, 111 (2017).
- [14] L. N. Rashkovish, *KDP-family Single Crystals*, Hilger Ed, Bristol, 202 (1991).
- [15] S. Balamurugan, P. Ramasamy, S. K. Sharna, Y. Inkong, P. Manyum, *Mater. Chem. Phys.* **117**, 465 (2009).
- [16] F. Barati, H. R. Dizaji, *Opt. Quant. Electron.* **48**, 432 (2016).
- [17] D. N. Nikogosyan, *Nonlinear Optical Crystals: A Complete Survey*, Springer, New York, USA, 430 (2005).
- [18] R. Robert, C. Raj, S. Krishnan, S. Das, *Physica B* **405**, 20 (2010).
- [19] D. Mei, J. Jiang, F. Liang, S. Zhang, Y. Wu, C. Sun, C. D. Xue, Z. Lin, *J. Mater. Chem. C* **6**, 2684 (2018).
- [20] Z. Lin, Z. Wang, C. Chen, *C. J. Chem. Phys.* **118**, (2003).
- [21] P. Kumaresan, S. M. Babu, P. M. Anbarasan, *J. Optoelectron. Adv. M.* **9**(9), 2774 (2007).
- [22] A. Yariv, P. Yeh, *Optical waves in crystals: propagation and control of laser radiation*, John Wileys & Son USA, 300 (1984).
- [23] R. Eckardt, R. Byer, *Proceedings of SPIE* **1561**, (1991).

\*Corresponding author: ptvinh@hcmus.edu.vn